Inorg. Chem. **2003**, *42*, 6484–6488

Coordination Polyhedron and Chemical Vapor Deposition of $Cu(hfacac)_2(t\text{-}BuNH_2)$

Kyoungja Woo,*,† Hojeong Paek,† and Wan In Lee‡

Nano-Materials Research Center, Korea Institute of Science and Technology, P.O. Box 131, Cheongryang, Seoul 130-650, Korea, and Department of Chemistry, Inha University, Inchon 402-752, Korea

Received April 3, 2003

A new pentacoordinate Cu(II) complex, $Cu(hfacac)_2(t\text{-}BuNH_2)$ [hfacac = $CF_3C(O)CHC(O)CF_3^-$, $t\text{-}BuNH_2$ = *tert*-butylamine], has been synthesized and structurally characterized. Interestingly, the structure of a single crystal occurred as square pyramidal with one O atom at the apical position and one N and three O atoms at the basal positions, showing a serious degree of distortion. This contrasts with the square-pyramidal structure of $Cu(hfacac)_2L$ (L = H_2O and pyrazine), which has the L ligand at the axial position. In the $Cu(hfacac)_2(t\text{-}BuNH_2)$ complex, the $t\text{-}BuNH_2$ ligand is placed at an equatorial position with a lowered angle by 19.9(2)° from the basal plane. This distortion seems to reduce σ^* influence and steric hindrance and so stabilizes the square-pyramidal geometry. This precursor has a lower melting point and superior stability to air, moisture, and heat than the $Cu(hfacac)_2(xH_2O)$ precursor. The deposition rate of copper oxide film on a Pt layer above 450 °C was nearly constant with increasing temperature, indicating a mass transport limited reaction. Therefore it would be a useful metal organic chemical vapor deposition precursor for the fabrication of copper oxide film or superconducting materials. Crystal data for $Cu(hfacac)_2(t\text{-}BuNH_2)$: 293(2) K, a = 9.6699(4) Å, b = 18.0831(10) Å, c = 12.8864(11) Å, β = 111.839(5)°, monoclinic, space group $P2_1/c$, Z = 4.

Introduction

An easy interconversion between trigonal-bipyramidal and square-pyramidal structure has been well-known in pentacoordinate complexes. The difference in energy between two idealized structures is so small that it leads to structural fluxionality. A typical example is $Ni(CN)_5^{3-}$, showing simultaneous occurrence of trigonal bipyramidal and square pyramidal forms in the same unit cell.[1] $Co(dpe)_2Cl^+$ [dpe = 1,2-bis(diphenylphosphino)ethane] cation[2] and $NiCl_2(PR_3)(P-N)$ [P−N = 2-(diphenylphosphino)aniline and its *N*-methyl derivatives] complex[3] can be isolated in two different molecular forms, square pyramidal or trigonal bipyramidal for each complex.

In the case of Cu(II), the structural fluxionality within pentacoordinate species has been an equally interesting subject. The pentacoordinate Cu(II) derivatives are mostly square pyramidal.[4] Various $Cu(hfacac)_2L$ complexes where hfacac is $CF_3C(O)CHC(O)CF_3^-$ and L is either a nitrogen or oxygen base have been characterized, being very useful precursors for metal−organic chemical vapor deposition (MOCVD) of copper or copper oxide film. In the case of L = H_2O, the $Cu(hfacac)_2L$ complex exists as a square pyramid with L at the apical position,[5] while when L = NH_3, $Cu(hfacac)_2L$ is a trigonal bipyramid with L at a basal position.[6] It was suggested[6] that the strong σ^* influence weakens the $Cu-L_{axial}$ bond and so the strong σ donor ligand, in general favor an equatorial position with trigonal bipyramidal geometry to reduce σ^* influence. The [Cu(bispictn)(NCS)]NCS [bispictn = 1,7-bis-(2-pyridyl)-2,6-diazaheptane] complex,[7] which has a strong σ donor ligand NCS^-, can be an additional example. Two conformational isomeric forms differing by a degree of distortion in the trigonal-bipyramidal geometry are observed with NCS at a basal position.

* Author to whom correspondence should be addressed. E-mail: kjwoo@kist.re.kr.

† Korea Institute of Science and Technology.

‡ Inha University.

(1) Raymond, K. N.; Corfield, P. W. R.; Ibers, J. A. *Inorg. Chem.* **1968**, *7*, 1362.

(2) Stalik, J. K.; Corfield, P. W. R.; Meek, D. W. *Inorg. Chem.* **1973**, *12*, 1668.

(3) Crociani, L.; Tisato, F.; Refosco, F.; Bandoli, G.; Corain, B. *Eur. J. Inorg. Chem.* **1998**, 1689.

(4) Melnik, M.; Kabesova, M.; Dunaj-Jurco, M.; Holloway, C. E. *J. Coord. Chem.* **1997**, *41*, 35.

(5) Pinkas, J.; Huffman, J. C.; Baxter, D. V.; Chisholm, M. H.; Caulton, K. G. *Chem. Mater.* **1995**, *7*, 1589.

(6) Pinkas, J.; Huffman, J. C.; Chisholm, M. H.; Caulton, K. G. *Inorg. Chem.* **1995**, *34*, 5314.

10.1021/ic034360+ CCC: $25.00
Published on Web 09/05/2003

Here we report a quite interesting result about the structure of Cu(hfacac)$_2$(*t*-BuNH$_2$) complex, which occurred as a distorted square pyramid with the *t*-BuNH$_2$ ligand at an equatorial position. We applied this complex to the fabrication of copper oxide film by liquid source metal organic chemical vapor deposition (LS-MOCVD) technique.

Experimental Section

General Procedures. Diethyl ether, toluene, and hexanes were distilled under nitrogen from sodium benzophenone ketyl. CuCl (Aldrich, 99+%), NaH (Aldrich, 95%), and $CF_3C(O)CH_2C(O)CF_3$ (Aldrich, 98%) were used as purchased. *t*-BuNH$_2$ (Aldrich, 99%) was distilled under nitrogen over KOH. Cu(hfacac)$_2$ was obtained from Cu(hfacac)$_2$(xH$_2$O) by double sublimation to remove H$_2$O. Cu(hfacac)$_2$(xH$_2$O) was synthesized by a literature method.[8]

The characterization of the synthesized complex was performed by UV−vis (Varian Cray 100 Conc) and Fourier transfrom (FT)-IR (Mattson IR 300) spectroscopy. The melting point was measured with an electrothermal melting-point apparatus. Elemental analysis was performed by the Advanced Analytical Center in the Korea Institute of Science and Technology. Thermal analysis was carried out by NETZSCH STA 409 PG/PC, with a heating rate of 10 °C/min in a nitrogen purge under ambient pressure.

Synthesis of Cu(hfacac)$_2$(*t*-BuNH$_2$), Method 1. Under nitrogen, 40 mL of diethyl ether solution containing 0.332 g (13.8 mmol) of NaH was prepared and kept at 0 °C. To this solution, 2.06 mL (14.6 mmol) of $CF_3C(O)CH_2C(O)CF_3$ was added slowly, and the mixture was brought to room temperature for 1 h, kept stirring for 2 h, and then cooled to 0 °C again (solution A). Meanwhile, another flask with 45 mL of diethyl ether solution containing 1.145 g (11.6 mmol) of CuCl was prepared and 1.27 mL (12.1 mmol) of *t*-BuNH$_2$ was added with stirring (solution B). At −10 °C, solution A was added to solution B and kept stirring for 3 h. Solvent was stripped from the solution, yielding a colorless residue. Excess hexanes were added to the residue to extract the Cu(hfacac)(*t*-BuNH$_2$) complex at −10 °C, but this colorless Cu(I) complex slowly turned into a green Cu(II) complex. The trial to separate the pure Cu(I) complex always turned out to be a mixture of white Cu(I) and green Cu(II) complexes. So, the extracted solution was stirred for several days at room temperature to convert the Cu(I) complex to the Cu(II) complex. This solution was filtered, concentrated, and refrigerated, yielding a green solid. More crops were obtained by repeating extraction with hexanes, filtration, concentration, and refrigeration. The combined green solid was recrystallized from hexanes. Yield: 2.187 g (68.6%). Sublime: 55−60 °C/2 × 10^{-2} mmHg. Mp: 99 °C. FT-IR (in benzene, cm^{-1}): 3313, 3253 (NH stretching), 1649, 1637 (coordinated CO stretching). FT-IR (KBr pellet, cm^{-1}): 3323, 3262 (NH stretching), 1676, 1639 (coordinated CO stretching). UV−vis (1.0 × 10^{-4} mol/L in CH$_3$CN) λ_{max} (log ϵ): 222 (3.94), 233 (3.94), 307 (4.32), 328 (sh) (5.00 × 10^{-2} mol/L in CH$_3$CN). λ_{max} (log ϵ): 405 (1.91), 789 (1.88). Anal. Calcd for $C_{14}H_{13}CuF_{12}NO_4$: C, 30.5; H, 2.38; N, 2.54; Cu, 11.5. Found: C, 30.7; H, 2.34; N, 2.48; Cu, 11.1.

Synthesis of Cu(hfacac)$_2$(*t*-BuNH$_2$), Method 2. Under nitrogen, 1.55 g (3.24 mmol) of Cu(hfacac)$_2$ was dissolved in 60 mL of toluene. To this solution, 0.34 mL (3.24 mmol) of *t*-BuNH$_2$ was added and stirred for 1 h. The resulting solution was concentrated and excess hexanes were added and refrigerated, yielding green solid. More crops were obtained by repeating filtration, concentration, and refrigeration. Combined yield: 1.74 g (97.8%). The physical and chemical properties of the green solid were exactly the same as those obtained from method 1.

Table 1. X-ray Crystallographic Data and Processing Parameters for Cu(hfacac)$_2$(*t*-BuNH$_2$) Complex

chemical formula	$C_{14}H_{13}NO_4F_{12}Cu$
fw	550.79
temp	293(2) K
wavelength	0.71070 Å
cryst syst, space group	monoclinic, $P2_1/c$
unit-cell dimensions	a = 9.6699(4) Å; α = 90°
	b = 18.0831(10) Å; β = 111.839(5)°
	c = 12.8864(11) Å; γ = 90°
vol	2091.6(2) Å^3
Z	4
D_{calcd}	1.749 g/cm^3
m	1.170 mm^{-1}
final R indices [$I > 2\sigma(I)$]	R1[a] = 0.0576, wR2[b] = 0.1590
R indices (all data)	R1[a] = 0.1032, wR2[b] = 0.1819

[a] $R1 = \sum||F_o| - |F_c||$ (based on reflections with $F_o^2 > 2\sigma F^2$). [b] $wR2 = \{\sum[w(F_o^2 - F_c^2)^2]/\sum[w(F_o^2)^2]\}^{1/2}$; $w = 1/[\sigma^2(F_o^2) + (0.095P)^2]$; $P = [\max(F_o^2, 0) + 2F_c^2]/3$ (also with $F_o^2 > 2\sigma F^2$).

Table 2. Typical Deposition Conditions for LS-MOCVD of the CuO Thin Films

Cu(hfacac)$_2$(*t*-BuNH$_2$) in *n*-butyl acetate	0.05 mol/L, 0.1 mL/min
Cu(hfacac)$_2$(xH$_2$O) in *n*-butyl acetate	0.05 mol/L, 0.1 mL/min
oxidizer (O$_2$/N$_2$) flow rate	200/100 mL/min
carrier (N$_2$) flow rate	100 mL/min
substrate temp	350−550 °C
vaporizer temp	260 °C
line heating temp	250 °C

Crystal Structure Determination. Green crystals of Cu(hfacac)$_2$(*t*-BuNH$_2$) were easily grown as hard solids by recrystallization from hexanes and mounted on the diffractometer in the air. Data were collected at 293(2) K and corrected for Lorentz and polarization effects. The structure was solved by the application of direct methods using the SHELXS-96 program,[9a] and least-squares refinement was solved using SHELXL-97.[9b] After anisotropic refinement of all non-H atoms, several H atom positions could be located in difference Fourier maps. These were refined isotropically while the remaining H atoms were calculated in idealized positions and included in the refinement with fixed atomic contributions. Further detailed information is listed in Table 1.

Fabrication of CuO Thin Films. MOCVD of CuO films using direct liquid injection method with a flash vaporizer was carried out with Cu(hfacac)$_2$(*t*-BuNH$_2$) and Cu(hfacac)$_2$(xH$_2$O) as precursors on the substrate of Pt/TiN/SiO$_2$/Si. The LS-MOCVD system is described previously.[10] The detailed LS-MOCVD condition is described in Table 2. The thickness of the film was measured via scanning electron microscopy (SEM; Hitachi S-4200). The X-ray diffraction (XRD) patterns were obtained with a Philips diffractometer (PW3020) using monochromated high-intensity Cu Kα radiation. The electron spectroscopy for chemical analysis (ESCA) survey data were obtained with a PHI 5700 ESCA system using Al mono 15 kV 350 W, after sputter etching the film surface about 100 Å with an Ar$^+$ beam.

Results and Discussion

Cu(hfacac)$_2$(*t*-BuNH$_2$) was prepared by both methods 1 and 2. Method 1 was originally aimed at the synthesis of

(7) (a) Bailey, N. A.; Mckenzie, E. D.; Mullins, J. R. *Chem. Commun*. **1970**, 1103. (b) Bailey, N. A.; Mckenzie, E. D. *J. Chem. Soc., Dalton Trans.* **1972**, 1566.
(8) Bertrand, J. Z.; Kaplan, R. I. *Inorg. Chem*. **1966**, *5*, 489.
(9) (a) Sheldrick, G. M. *Acta Crystallogr., Sect. A* **1990**, *A46*, 467. (b) Sheldrick, G. M. *SHELXL: Program for Crystal Structure Refinement*; University of Göttingen: Göttingen, Germany, 1997.
(10) Woo, K.; Lee, W. I.; Lee, J. S.; Kang, S. O., *Inorg. Chem.* **2003**, *42*, 2378.

the Cu(I) complex, Cu(hfacac)(*t*-BuNH$_2$), but the synthesized Cu(hfacac)(*t*-BuNH$_2$) proceeded further reaction by disproportionation, yielding Cu(hfacac)$_2$(*t*-BuNH$_2$) according to eq 1. That is, the colorless solid began to show green color slowly after the addition of hexanes, and the color change rate became faster with increasing temperature.

$$Cu^{I}(hfacac)(t\text{-}BuNH_2) + Cu^{I}(hfacac)(t\text{-}BuNH_2) \rightarrow Cu^{II}(hfacac)_2(t\text{-}BuNH_2) + Cu^{0} + t\text{-}BuNH_2 \quad (1)$$

The irreversible disproportionation reaction of Cu(I) complexes is well-known[11] in the chemical vapor deposition process of Cu(0) and recently is reported[12] as a method to deposit a Cu(0) layer for device interconnects from a solution.

The synthesis of Cu(hfacac)$_2$(*t*-BuNH$_2$) from Cu(hfacac)$_2$ and *t*-BuNH$_2$ by method 2 was neat and complete. There was no sign of Cu(hfacac)$_2$(*t*-BuNH$_2$)$_2$ formation even in excess of *t*-BuNH$_2$. It seems reasonable since the additional bulky *t*-BuNH$_2$ group will cause serious structural congestion around the Cu(II) ion.

Electronic spectra of Cu(hfacac)$_2$(*t*-BuNH$_2$) in acetonitrile solution showed two separated bands in the visible region, at 405 and 789 nm with log $\epsilon = 1.91$ and 1.88, respectively. This contrasts with the case of Cu(hfacac)$_2$L (L = H_2O, NH_3), which has only one band in the visible region.[6] It is thought[13] that the geometry of Cu(hfacac)$_2$(*t*-BuNH$_2$) is pentacoordinate square pyramidal and the splitting of t_{2g} and e_g orbitals each is important, while the others are close to hexacoordinate octahedral by solvent coordination and the degeneracy of the orbitals are not disturbed in acetonitrile solution. The steric bulkiness and strong σ donating property of the *t*-BuNH$_2$ ligand seem to cause the splitting of the degenerated energy levels.

The IR spectrum of the Cu(hfacac)$_2$(*t*-BuNH$_2$) complex in benzene solution showed red shift compared with that in the solid KBr pellet as shown in Figure 1, especially the CO asymmetric stretching band that showed a considerable red shift (27 cm^{-1}). It is a manifest that the stronger Cu−O bonding in the solution contributes to the weakening of the corresponding CO bonding by back-donation from a metal−ligand π^* orbital.[14] It is considered that the origin of stronger Cu−O bonding comes from the partial structural transformation, from square pyramidal to trigonal bipyramidal. Generally, it is known[4] that the Cu−L$_{axial}$ bond is longer than the Cu−L$_{equatorial}$ bond in square pyramidal while the opposite is true in trigonal-bipyramidal geometry. In the pentacoordinate Cu(II) complexes, the generalized order[4] of bond length is Cu−L$_{axial}$ (square pyramidal) > Cu−L$_{equatorial}$ (trigonal bipyramidal) > Cu−L$_{equatorial}$ (square pyramidal) ≅ Cu−L$_{axial}$ (trigonal bipyramidal) and the order of the corresponding CO bond length is opposite. The N−H stretching bands are sharp and showed a negligible shift, indicating the least hydrogen-bonding effect in both solid and solution. This is quite different from the cases of Cu(hfacac)$_2$L (L = H_2O, NH_3), which are showing hydrogen-bonded dimeric units in the solid state.[6]

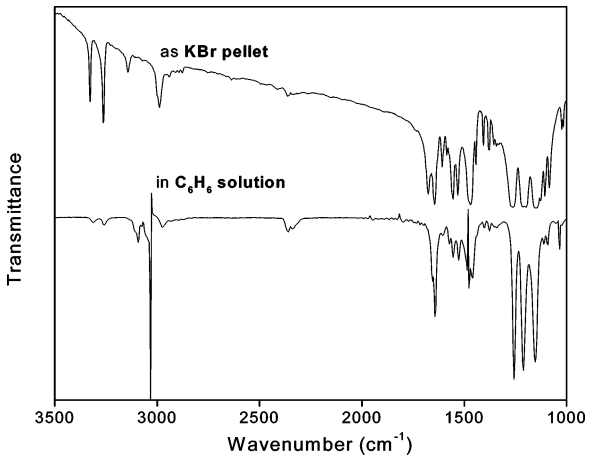

Figure 1. IR spectra of Cu(hfacac)$_2$(*t*-BuNH$_2$).

Table 3. Selected Interatomic Bond Lengths (Å) for Cu(hfacac)$_2$(*t*-BuNH$_2$)

Cu(1)−O(4)	1.941(3)	Cu(1)−O(1)	1.953(3)
Cu(1)−N(1)	1.992(4)	Cu(1)−O(3)	1.992(3)
Cu(1)−O(2)	2.222(4)	O(1)−C(1)	1.273(5)
O(2)−C(3)	1.225(6)	O(3)−C(6)	1.245(6)
O(4)−C(8)	1.241(6)	N(1)−C(11)	1.519(6)

Table 4. Selected Bond Angles (deg) for Cu(hfacac)$_2$(*t*-BuNH$_2$)

O(4)−Cu(1)-O(1)	179.02(14)	O(4)−Cu(1)-N(1)	88.2(2)
O(1)−Cu(1)-N(1)	92.8(2)	O(4)−Cu(1)-O(3)	90.33(14)
O(1)−Cu(1)-O(3)	88.86(14)	N(1)−Cu(1)-O(3)	160.1(2)
O(4)−Cu(1)-O(2)	89.65(14)	O(1)−Cu(1)-O(2)	89.75(13)
N(1)−Cu(1)-O(2)	114.2(2)	O(3)−Cu(1)-O(2)	85.65(15)
C(1)−O(1)-Cu(1)	125.4(3)	C(3)−O(2)-Cu(1)	121.2(3)
C(6)−O(3)-Cu(1)	123.2(3)	C(8)−O(4)-Cu(1)	125.2(3)
C(11)−N(1)-Cu(1)	123.1(3)		

Crystallographic data and structure of Cu(hfacac)$_2$(*t*-BuNH$_2$) are shown in Tables 3 and 4 and Figure 2. The geometry of the Cu(hfacac)$_2$(*t*-BuNH$_2$) complex is of intermediate type but may be most conveniently described in terms of a distorted square pyramid with an O atom at the axial position and one N and three O atoms at the equatorial position. It was generally proposed[15] that trigonal-bipyramidal geometry might be the most common ground state except in cases where there may be some ligand stabilization of the square-pyramidal arrangement. In Cu(II) complexes, square-pyramidal structure has been regarded as the more stable geometry. Indeed, the pentacoordinate derivatives of Cu(II) are mostly square pyramidal with various degrees of distortion.[4]

(11) (a) Jain, A.; Chi, K.-M.; Kodas, T. T.; Hampden-Smith, M. J.; Farr, J. D.; Paffett, M. F. *Chem. Mater*. **1991**, *3*, 995 and references therein. (b) Jain, A.; Chi, K.-M.; Kodas, T. T.; Hampden-Smith, M. J. *J. Electrochem. Soc*. **1993**, *140*, 1434. (c) Chi, K.-M.; Hou, H.-C.; Hung, P.-T.; Peng, S.-M.; Lee, G.-H. *Organometallics* **1995**, *14*, 2641. (d) Naik, M. B.; Gill, W. N.; Wentorf, R. H.; Reeves, R. R. *Thin Solid Films* **1995**, *262*, 60. (e) Chi, K. M.; Corbitt, T. S.; Hampden-Smith, M. J.; Kodas, T. T.; Duesler, E. N. *J. Organomet. Chem*. **1993**, *449*, 181.

(12) Ho, P. K. K.; Gupta, S.; Zhou, M. S.; Chooi, S. US 6261954.

(13) Basolo, F.; Johnson, R. C. *Coordination Chemistry*; The Benjamin/Cummings Pub. Co.; Menlo Park, CA, 1964.

(14) Douglas, B.; McDaniel, D. H.; Alexander, J. J. *Concepts and Models of Inorganic Chemistry*, 2nd ed.; John Wiley & Sons. Inc.: New York, 1983.

(15) Hoskins, B. F.; Whillans, F. D. *Coord. Chem. Rev*. **1972**−**1973**, *9*, 365.

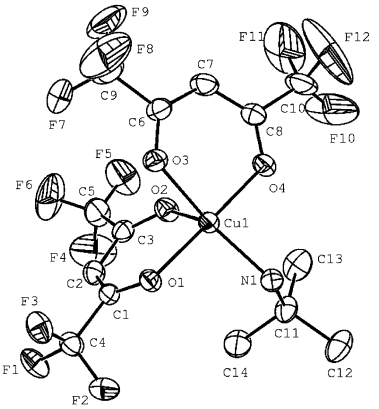

Figure 2. Representation of the X-ray crystal structure of Cu(hfacac)$_2$(*t*-BuNH$_2$), showing 30% probability thermal ellipsoids.

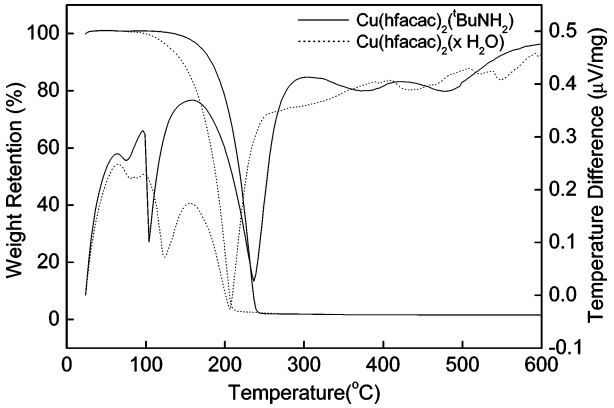

Figure 3. Thermal analysis curves of Cu(hfacac)$_2$(*t*-BuNH$_2$) and Cu(hfacac)$_2$(*x*H$_2$O) precursors with heating rate of 10 °C/min in a nitrogen purge under ambient pressure.

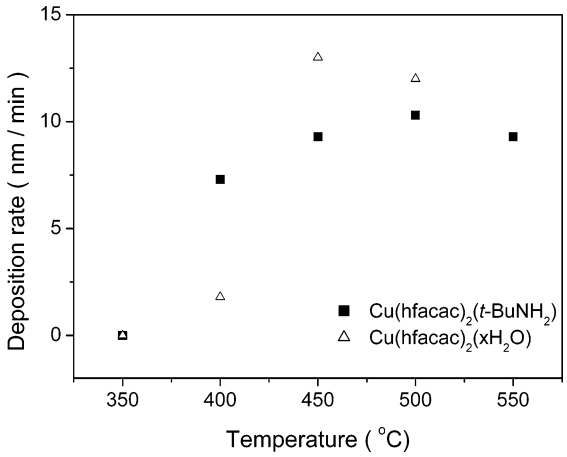

Figure 4. Deposition rates of the CuO films at various deposition temperatures; Cu(hfacac)$_2$(*t*-BuNH$_2$) and Cu(hfacac)$_2$(*x*H$_2$O) 0.05 mol/L in *n*-butyl acetate/260 °C.

Interestingly, apart from most square-pyramidal Cu(hfacac)$_2$L complexes, the *t*-BuNH$_2$ ligand in Cu(hfacac)$_2$(*t*-BuNH$_2$) is placed at a basal position and the Cu(1) atom is placed on the plane composed of O(1), O(3), and O(4) atoms. The basal N(1) atom is lowered downward from the equatorial plane by about 19.9(2)°, and the apical O(2) atom is tilted toward the basal plane by O(3)Cu(1)O(2) = 85.65(15)°. This is quite abnormal since it has been generally known[4] that ligand L is placed at the axial position and the Cu(II) atom is displaced toward apical ligand from the basal plane in the square-pyramidal geometry, and the displacement of Cu(II) atom ranges up to 0.53 Å when the apical ligand is an oxygen donor. The position and displacement of the N atom can be explained as follows using Pinkas et al.'s proposition[6] and steric effect. The *t*-BuNH$_2$ is a strong σ donor ligand and the σ^* influence from the filled z^2 orbital will weaken the Cu−N bond seriously if *t*-BuNH$_2$ is at the apical position in square pyramidal geometry. So, *t*-BuNH$_2$ is placed at a basal position, and at this time with a lowered angle [N(1)Cu(1)O(3) = 160.1(2)°] to reduce σ^* interaction from the filled $x^2 - y^2$ orbital to three basal O atoms and bent away from the upright standing hfacac ligand to reduce van der Waals repulsion [O(4)Cu(1)N(1) = 88.2(2)° and O(1)Cu(1)N(1) = 92.8(2)°]. The apical O atom is also tilted toward the basal plane [O(3)Cu(1)O(2) = 85.65(15)°] to reduce van der Waals repulsion with a lifted *tert*-butyl group. The displacement of the N atom and the direction of *tert*-butyl group seem to be determined as a compromising point to maximize the crystal packing[15] and to minimize the steric repulsion.

The Cu(II)−L_{apical} bond length is 2.222(4) Å, and the Cu(II)−L_{basal} bond length ranges from 1.941(3) to 1.992(4) Å. This agrees with the general observation[4] that the mean Cu−$L_{equatorial}$ bond distances are shorter than the mean Cu−L_{apical} bond distances in a series of square-pyramidal derivatives.

The thermal analysis result of Cu(hfacac)$_2$(*t*-BuNH$_2$) and Cu(hfacac)$_2$(*x*H$_2$O) is shown in Figure 3. The differential thermal analysis curves indicate that the melting point and boiling point of Cu(hfacac)$_2$(*t*-BuNH$_2$) are about 100 and 230 °C and those of Cu(hfacac)$_2$(*x*H$_2$O) are around 125 and 200 °C, respectively. No additional peak was found above 250 °C for either complex. At the same time, no appreciable weight change is observed from the thermogravimetric thermogram. The residual sample after a programmed heat in a nitrogen environment was zero. Thus, it is suggested that the Cu(hfacac)$_2$(*t*-BuNH$_2$) complex is stable during the flash evaporation process.

The Cu(hfacac)$_2$(*t*-BuNH$_2$) precursor is slightly inferior in volatility and superior in stability to air, moisture, and heat to Cu(hfacac)$_2$(*x*H$_2$O) precursor. The solubility of Cu(hfacac)$_2$(*t*-BuNH$_2$) in organic solvents, such as hexanes, *n*-butyl acetate, and toluene, is high enough for LS-MOCVD. This precursor retains its ligand intact while the Cu(hfacac)$_2$(*x*H$_2$O) complex loses H$_2$O ligand, during vacuum sublimation. In addition, Cu(hfacac)$_2$(*t*-BuNH$_2$) shows an extended stability at 260 °C, a typical vaporization temperature, and demonstrates complete vaporization at this temperature.

The deposition rate of CuO thin films with Cu(hfacac)$_2$(*t*-BuNH$_2$) complex was monitored as a function of deposition temperature, as shown in Figure 4. The vaporization temperature was adjusted to 260 °C based on differential thermal analysis data. After several runs, there was no residue on the vaporizer in any case. In comparison, Cu(hfacac)$_2$(*x*H$_2$O) was also applied for the deposition of CuO thin films. The deposition rate with the Cu(hfacac)$_2$(*t*-BuNH$_2$) complex showed mass flow limited reaction,[16] which is useful for the

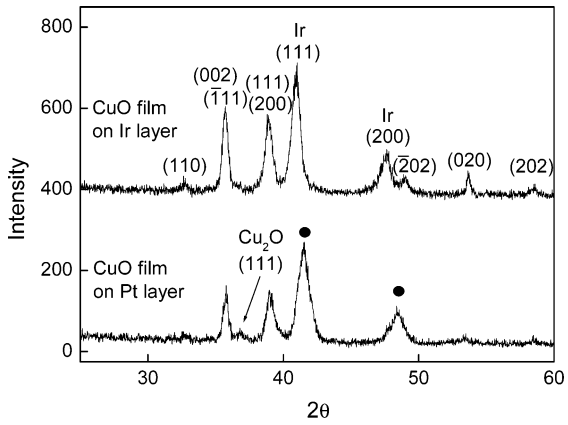

Figure 5. XRD patterns of the CuO films deposited on Pt and Ir layer at 450 °C; the thickness of Pt and Ir layer was 200 nm, respectively. The unidentified peaks (●) are considered to be from (111)s and (200)s of CuPt and Cu_3Pt alloys.

easy control of stoichiometry in the fabrication of a composite film. A slightly higher deposition rate with the $Cu(hfacac)_2(xH_2O)$ complex above 400 °C is believed to be caused by an H_2O ligand, where the water protons are known to be an important participant in the chemical vapor deposition chemistry.[5,17] Meanwhile, the deposition rate at lower temperatures is higher with $Cu(hfacac)_2(t\text{-}BuNH_2)$ complex. At 400 °C, the deposition rate of CuO film with $Cu(hfacac)_2(t\text{-}BuNH_2)$ was about 4 times that with the $Cu(hfacac)_2(xH_2O)$ complex. Moreover, the deposition rate with this new precursor was relatively constant, throughout the deposition temperature between 400 and 550 °C.

XRD patterns of the CuO films prepared from the $Cu(hfacac)_2(t\text{-}BuNH_2)$ complex at 450 °C are shown in Figure 5. The films deposited on the Pt layer are monoclinic CuO phase with a slight impurity of cubic Cu_2O phase.[18] In addition, the unidentified peaks (●) at 41.5 and 48.4°, which are regarded as closely overlapped (111)s and (200)s of CuPt[19] and Cu_3Pt[20] alloys, are observed. We guess that in the initial stage of chemical vapor deposition, the delivered Cu source on the surface of Pt layer makes an interfacial layer, before CuO phase is formed. CuO films were also deposited at the same condition on Ir layer, which has been known as an excellent diffusion-barrier material. On the Ir layer, pure monoclinic CuO phase was formed without any impurity phase.

The CuO films fabricated from the $Cu(hfacac)_2(t\text{-}BuNH_2)$ precursor at various temperatures were investigated for contamination by C, N, and F using ESCA. All the ESCA survey spectra showed negligible amount of C, N, and F contamination (Supporting Information). Notably, the C contamination was below 1.72, 0.85, and 1.09% at 450, 500, and 550 °C, respectively.

Therefore, the $Cu(hfacac)_2(t\text{-}BuNH_2)$ complex is believed to be a good MOCVD precursor for the films of CuO or mixed metal oxides containing Cu, such as $YBa_2Cu_3O_7$ and $CuFe_2O_4$.

Conclusions

The $Cu^{II}(hfacac)_2(t\text{-}BuNH_2)$ complex has been synthesized by disproportionation reaction of $Cu^{I}(hfacac)(t\text{-}BuNH_2)$ complexes and/or by adding $t\text{-}BuNH_2$ to $Cu^{II}(hfacac)_2$ complex. X-ray crystallographic structure of a single crystal for $Cu(hfacac)_2(t\text{-}BuNH_2)$ complex reveals a distorted square pyramid. An O atom is placed at the apical position with tilting toward the equatorial plane, and one N and three O atoms are located at the basal positions with the N atom lowered downward from the basal plane and bent away from the standing hfacac ligand. This geometry is believed to be chosen to reduce σ^* influence and van der Waals repulsion and for effective crystal packing. $Cu(hfacac)_2(t\text{-}BuNH_2)$ is a good MOCVD precursor for the fabrication of CuO film due to its low melting point; stability to air, moisture, and heat; and good volatility with mass flow limited deposition mechanism.

Acknowledgment. This research has been conducted under the Future Key Technology program sponsored by the Ministry of Science and Technology in Korea. We thank Prof. Sang Ook Kang for the X-ray crystallographic data.

Supporting Information Available: The ESCA data of the CuO films fabricated from the $Cu(hfacac)_2(t\text{-}BuNH_2)$ complex, the crystal data of $Cu(hfacac)_2(t\text{-}BuNH_2)$, and one X-ray crystallographic file in CIF format. This information is available free of charge via the Internet at http://pubs.acs.org.

IC034360+

(16) (a) Son, J.-H.; Park, M.-Y.; Rhee, S.-W. *Thin Solid Films* **1998**, *335*, 229. (b) Rhee, S.-W.; Kang, S.-W.; Han, S.-H. *Electrochem. Solid-State Lett*. **2000**, *3*, 135. (c) Kang, S.-W.; Park, M.-Y.; Rhee, S.-W. *Electrochem. Solid-State Lett*. **1999**, *2*, 22.
(17) Pinkas, J.; Huffman, J. C.; Bollinger, J. C.; Streib, W. E.; Baxter, D. V.; Chisholm, M. H.; Caulton, K. G. *Inorg. Chem*. **1997**, *36*, 2930.
(18) JCPDS-International Center for Diffraction Data, File No. 41-254 for CuO, File No. 5-667 for Cu_2O, File No. 6-598 for Ir, 1995.
(19) Nekrasov, I.; Ustinov, V. *Dokl. Acad. Sci. U. S. S. R., Earth Sci. Sec. (Engl. Transl.)* **1993**, *328*, 128.
(20) Schneider, A.; Esch, U. *Z. Elektrochem. Angew. Phys. Chem*. **1944**, *50*, 290.